Results

Preprocessing

Dimension reduction through low-variance and biotype filtering

All the TCGA and THCA expression data were checked for NAs, which were subsequently deleted. Genes with a variance lower than 0.1 were removed to reduce dimensionality, as they contribute very little to the overall variance of the data set and are most likely house-keeping genes (xxx Quelle oder löschen). The low-variance filtering of the THCA data set was done in a similar way. Genes with a lower variance than 0.06 were deleted in the tumor tissue and the normal tissue data. To reduce dimensionality further, the biotype of the hallmark pathway genes was determined, which was almost exclusively protein coding. To match this, only protein coding pathways were kept in all expression data sets for further analysis. Doing so, the number of genes in the pan-caner data set was reduced from 60,000 to approximately 19,000 genes and from approximately 20,000 genes to 15,000 genes in the THCA data.

MSigDB pathway filtering

The pathways from the MSigDB database were first aligned with the genes in our expression data. Only pathways with a coverage of over 99% were kept. To test for similarity in the selected metabolic pathways compared to the hallmark pathways and the metabolic pathways themselves, the Jaccard index between all pathways was calculated. A few MSigDB pathways with a high Jaccard index were identified and subsequently deleted. Heatmaps, displaying the jaccard index of cleaned and uncleaned data can be seen in the appendix ~**??** @ref(fig:Jaccardcleaned). The number of MSigDB pathways could thus be reduced from 6366 to 657.

Descriptive analysis

Mean-variance plot of TCGA expression data shows highly variant genes.

To determine the genes from the TCGA expression data with a high variance, the variance was plotted over the mean (Figure 1). Additionally those genes with a variance higher than 33 were labeled with their EnsembleID. The distribution of genes in this plot shows that the highly variant genes are around a log2 mean expression level of 0. The plot also shows, that very few genes are at a low mean expression level or at a very high mean expression level. Most genes are expressed across all patients at a log2 mean expression level of approximately 0. With this plot we were able to determine which genes differ significantly in their expression level across all cancer patients.

Significantly up- and down regulated genes in THCA obtained from volcano plots

To determine up- or down-regulated genes in THCA corresponding p-Values were computed with a Wilcoxon rank sum test. (Figure @ref(fig:showvolcanoplot)). The significance level was adjusted to 1.755e-06 with a Bonferroni adjustment.

Pan cancer analysis

GSVA of TCGA expression data reveals four clusters of cancer types.

A gene activity matrix was computed as described in section (methods). The obtained pathway activity matrix was visualised in a heatmap.

To find general clusters in the heatmap, the mean expression of each gene in each tumor type was generated and clustered hierarchically. Figure @ref(fig:meanexp) and @ref(fig:exp)

The tumor types were clustered based on their mean pathway activity and formed four clusters correlating with their histological type. The first cluster contains mainly adenocarcinamas, while the second one contains
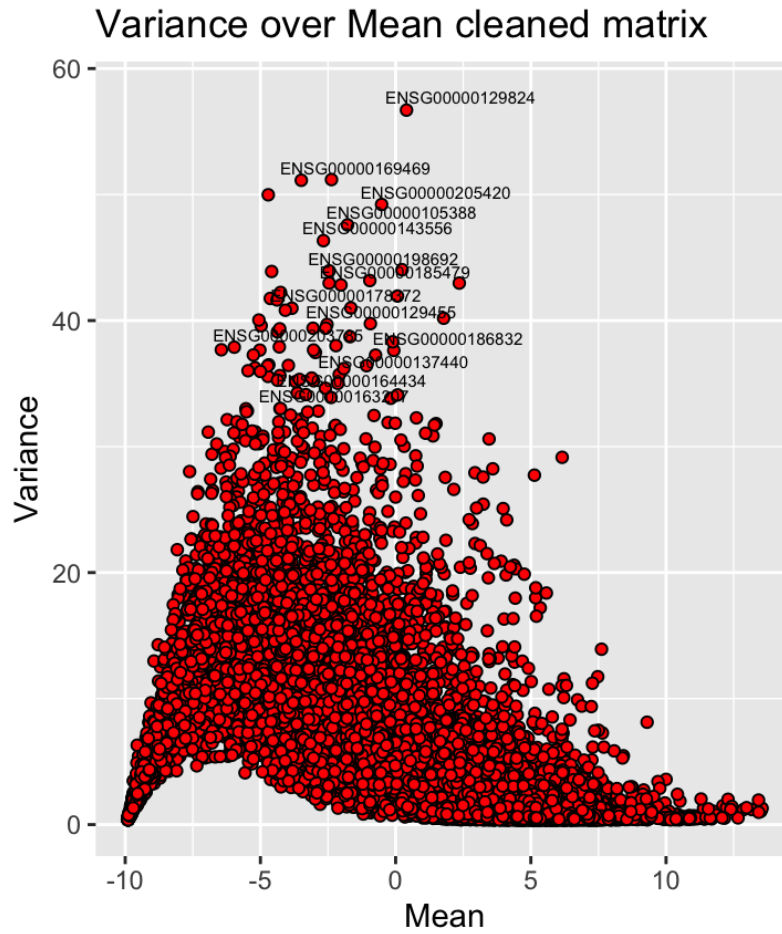
Figure 1: Mean-variance plot of cleaned TCGA expression data. Y-axis shows variance of a gene expression, x-axis shows the log2 mean of a gene expression. Genes with variance greater 33 are labelled with their ENSEMBL-ID
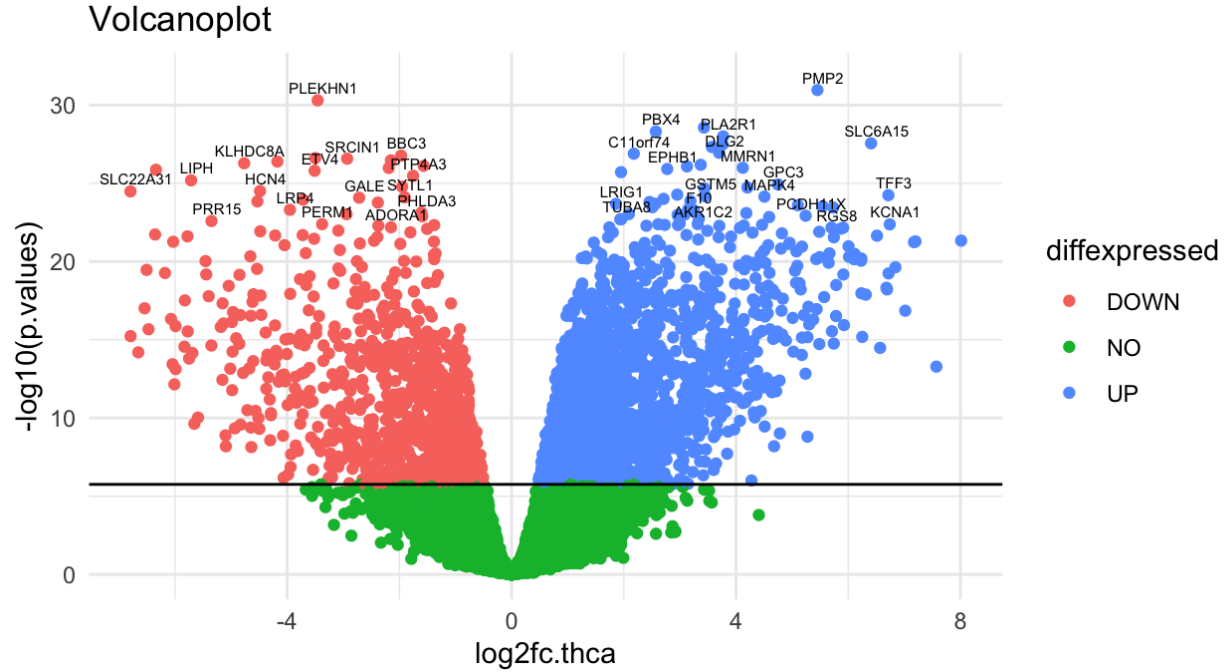
Figure 2: Volcano plot of THCA expression data. Downregulated genes are colored red, upregulated genes blue. Not significantly altered genes are colored green. Most significantly altered genes are labelled with their gene symbol

predominately glioblastomas. Leukemias are only found in the third cluster and the last cluster is enriched with sarcomas and carcinomas. Melanomas appear in the second and fourth cluster. Furthermore, three observations were made regarding specific information about pathway activity.

Pathways, which are important for nucleus import and export like Nasopharygeal carcinoma (NPC) and Ran shuttle pathways, as well as pathways for transcription regulaturs in embryonic stem cells are down-regulated in glioblastoma and adenocarcinoma. However, these pathways are up-regulated in all other histological types @ref(fig:meanexp).

Another observation is the clustering of glioblastoma. Pathways initiating neurogenesis and pathways linked to differentiation of the neural crest are up-regulated only in glioblastoma [@result6]. Two other pathways, that are up-regulated in glioblastoma cells are pathways linked to the activity of tyrosine kinases. The up-regulation of tyrosine kinases promote cell growth and proliferation. [@cell]. Taken together these two observations are in line with the expected high proliferation rate commonly found in glioblastoma.

The third cluster is mainly related to adenocarcinomas, more specifically liver hepatocellular carcinoma (LIHC), kidney renal papillary cell carcinoma (KICH) and kidney renal clear cell carcinoma (KIRC). The up-regulated pathways are involved in metabolism of carbohydrates, synthesis of lipids, synthesis of amino acids and detoxification. An up-regulation of all of these pathways may lead to cell growth and proliferation, due to higher metabolic activity, providing more biomass and energy.

Dimension reduction of GSVA pan-cancer data reveals clusters in pathway activity.

PCA was performed on GSVA pan-cancer for UMAP analysis. No apparent clustering was observed only in PCA data (compare Figure @ref(fig:PCAcancerform) @ref(fig:PCAcancertype)). Subsequent UMAP analysis however, showed clear clusters for most cancer types. @ref(fig:UMAPPanType) @ref(fig:UMAPPanForm). This complements the results obtained from our heatmap and reassures, that the tumor types have characteristic pathway activities. However, some cancers cluster better with their histological type rather than tumor type. This was observed mainly for carcinomas like squamous cell carcinoma and transitional cell
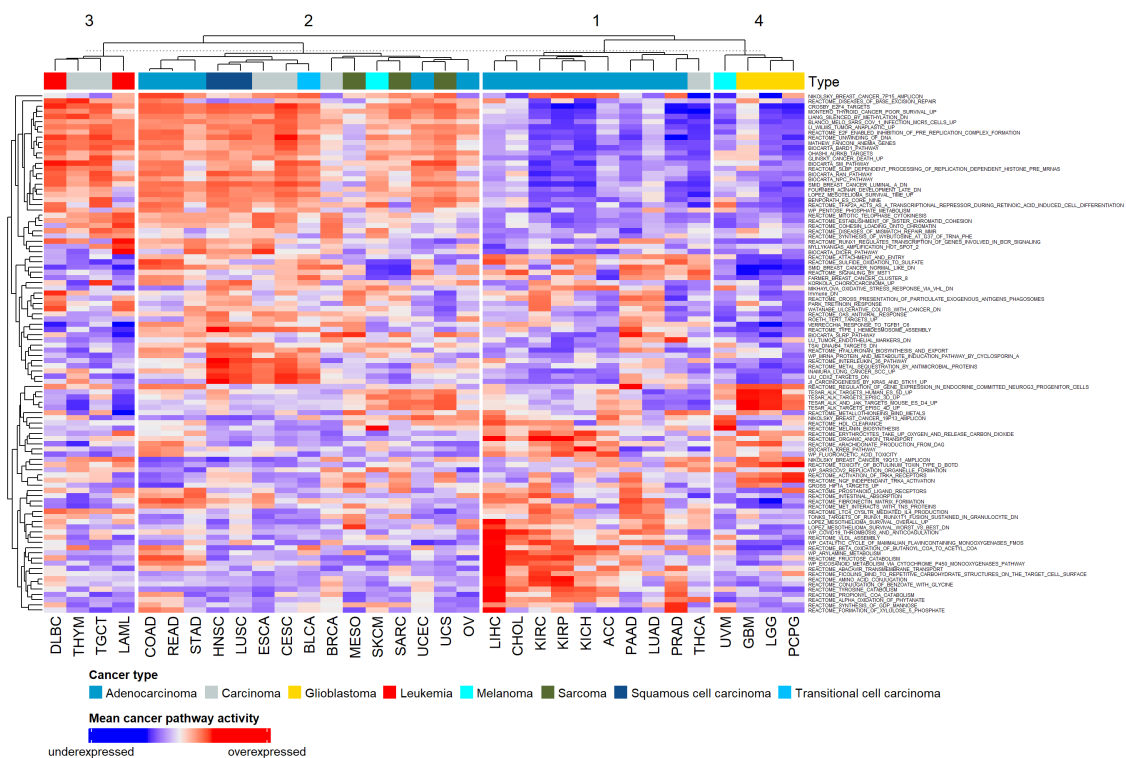
Figure 3: Mean pathway activity of the 100 most variant pathways for each tumor type. Column clusters were obtained by complete hierachical clustering and subsequently split into four groups. Pathway activities were computed via GSVA of pan-cancer expression data. For all pathway activities see figure (XXX in the apendix).

Figure 4: Pathway activity of the 100 most variant pathways for each patient. Column and row clusters were obtained by complete hierachical clustering. Pathway activities were computed via GSVA of pan-cancer expression data. For all pathway activities see figure (XXX in the apendix).

carcinoma, as well as sarcoma, lung adenocarcinoma and ovarian cancer. These are the same histological types that proofed difficult to cluster in the mean GSVA of TCGA expression. The UMAP confirmed the assumption, that the histological type of a tumor has a major impact on the patients gene expression profile.
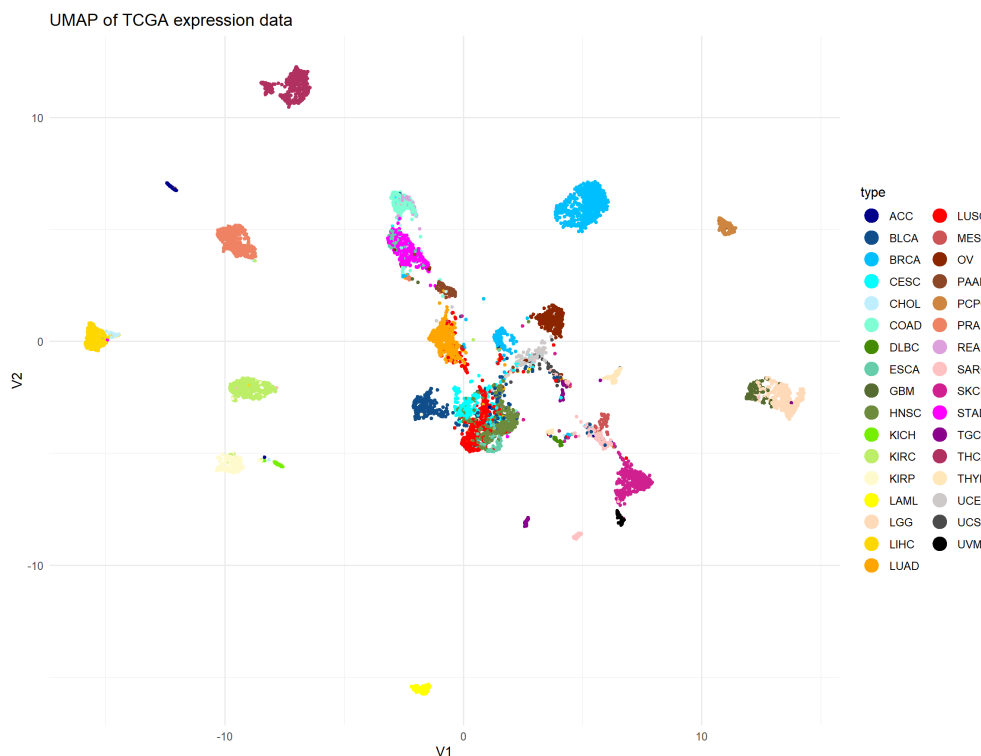

Figure 5: UMAP of TCGA pathway activity, colored by tumor type

The same analysis was performed for gene expression activity instead of pathway activity to check for reliability of the results. Similar clusters were observed, which confirms our results. See @ref(fig:UMAPGenform), @ref(fig:UMAPGen) in the appendix.

Focused analysis

GSVA on THCA expression data reveals pathways driving thyroid carcinogenesis.

To grasp a general overview of the differences in pathway activity between THCA and homeostatic thyroid tissue, GSVA was performed for the THCA expression data. Then, changes in pathway activity were computed by log2 fold change and the respective p-values were computed by a Wilcoxon rank-sum test. The most significantly altered pathways were then characterized. @ref(fig:THCAvolcano) Most prominently among them were pathways linked to proliferative signaling such as upregulation of p53 inhibitory proteins and hedgehog pathway activating Gli proteins. Further, the alpha6beta4 integrin signaling pathway and associated pathways such as IL-36 signaling and Typ I hemidesmosome synthesis were significantly enhanced in THCA. Further, signaling through the EWSR1/FLI1-fusion protein was significantly upregulated in THCA. Lastly, THCAs showed downregulation of non-histone protein methylation.

Pan-cancer data GSVA reveals three subtypes of THCA altering in proliferative signaling.

To investigate potential subtypes of THCA, the respective samples were taken from the pan-cancer GSVA data. The optimal number of clusters was determined by an elbow plot and subsequent K-means clustering revealed a total of three subtypes in THCA @ref(fig:THCAhm). This is consistent with the three clusters of THCA observed in the full pan-cancer GSVA data. The follicular histological type was enriched in cluster

Figure 6: UMAP of TCGA pathway activity, colored by histological type

Figure 7: Volcano plot of THCA pathway activity. Downregulated pathways are colored red, upregulated pathways blue. Not significantly altered pathways are colored green. Most significantly altered pathways are labelled with their name.

B, with no tall cell types present in this cluster. Judging from histological type alone no difference in clusters A and C was observed. Most significant changes in pathway activity were observed in pathways concerning proliferative signaling. In comparison with all other tumor types, cluster A displayed high activity of RAS, JAK/STAT and EWSR1/FL1-fusion mediated signaling as well as elevated signatures associated with carcinogenesis driven by alpha6beta4 activity. In contrast, these pathways were downregulated in cluster B, with it showing elevated activity in mTOR, MAPK, PI3K, and EGFR signaling cascades. Cluster C was found to upregulate all the aforementioned forms of proliferative signaling. All clusters showed a homogenous upregulation of hedgehog, ERBB2, and MST1 pathway activity. Regarding immune response, cluster C showed no significant alterations in the respective hallmark pathways, however, these pathways were downregulated in both clusters A and B. With this data, we can identify two seemingly different forms of proliferative signaling driving carcinogenesis in THCA. These forms can either occur separately as in the case of clusters A and B or combined as for cluster C.
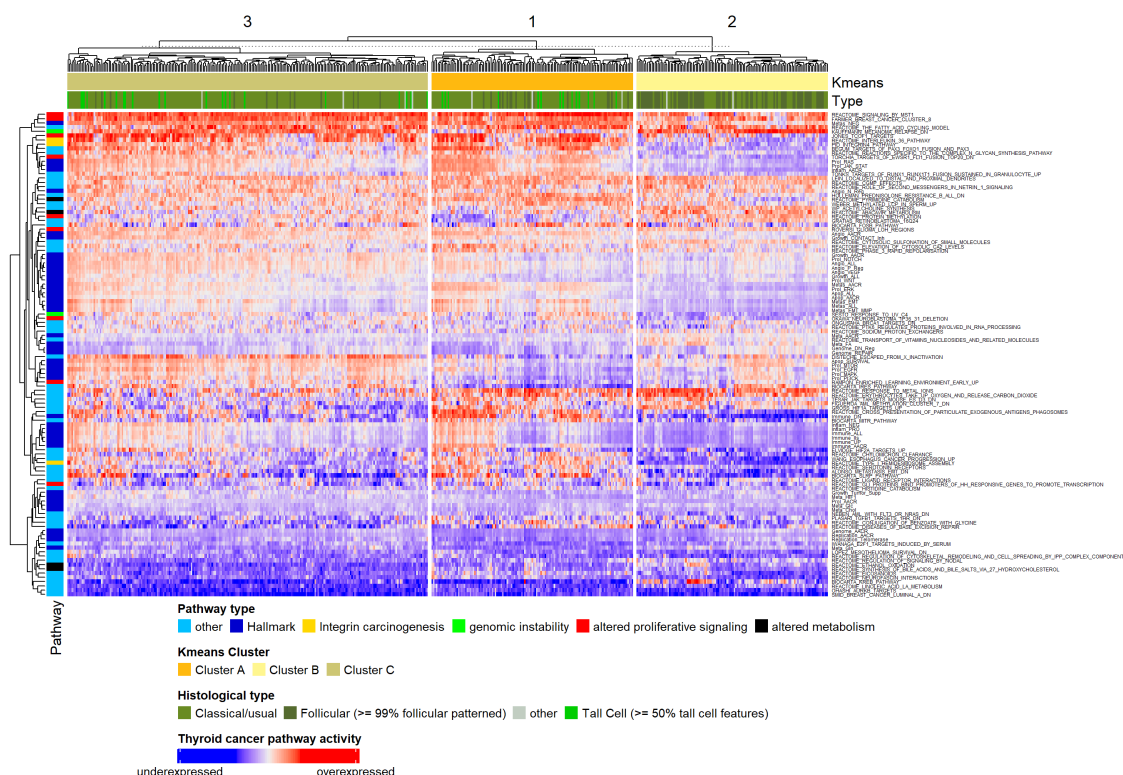

Figure 8: Pathway activity of the 50 most variant, hallmark, and 20 most significantly altered pathways for each patient. Column clusters were obtained by k-means clustering with k=3. Pathway activities were computed via GSVA of pan-cancer expression data. For all pathway activities see figure (XXX in the apendix).

THCA subtypes do not differ in their metabolism.

To investigate how the identified subtypes compare to homeostatic thyroid tissue, GSEA was performed for the THCA data. Consistent with the pan-cancer analysis of THCA data, k-means clustering obtained three different clusters in pathway activity – verified as the optimal number of clusters via an elbow plot. All clusters showed a similar change in metabolism @ref(fig:THCAhmGSEA). Catabolic pathways are downregulated whereas anabolic pathways e.g., fatty acid synthesis show increased activity in comparison with normal tissue. Further, the results seem consistent with the proliferative signaling activities found previously. Alpha6beta4, RAS, JAK/STAT, and EWSR1/FL1-fusion mediated signaling is upregulated in clusters one and three with low expression in cluster two. However, the upregulation of mTOR, MAPK, PI3K, and EGFR signaling in clusters two and three was observed only in some samples. Regarding, immune response

the expression profiles are again consistent with differences observed in the GSVA pan-cancer data: Both clusters one and two show a lower immune response compared to cluster three. From these GSEA results, we can conclude that the three subtypes of THCA differ in carcinogenesis and associated immune response but share a similar metabolism consistent with the Warburg effect.
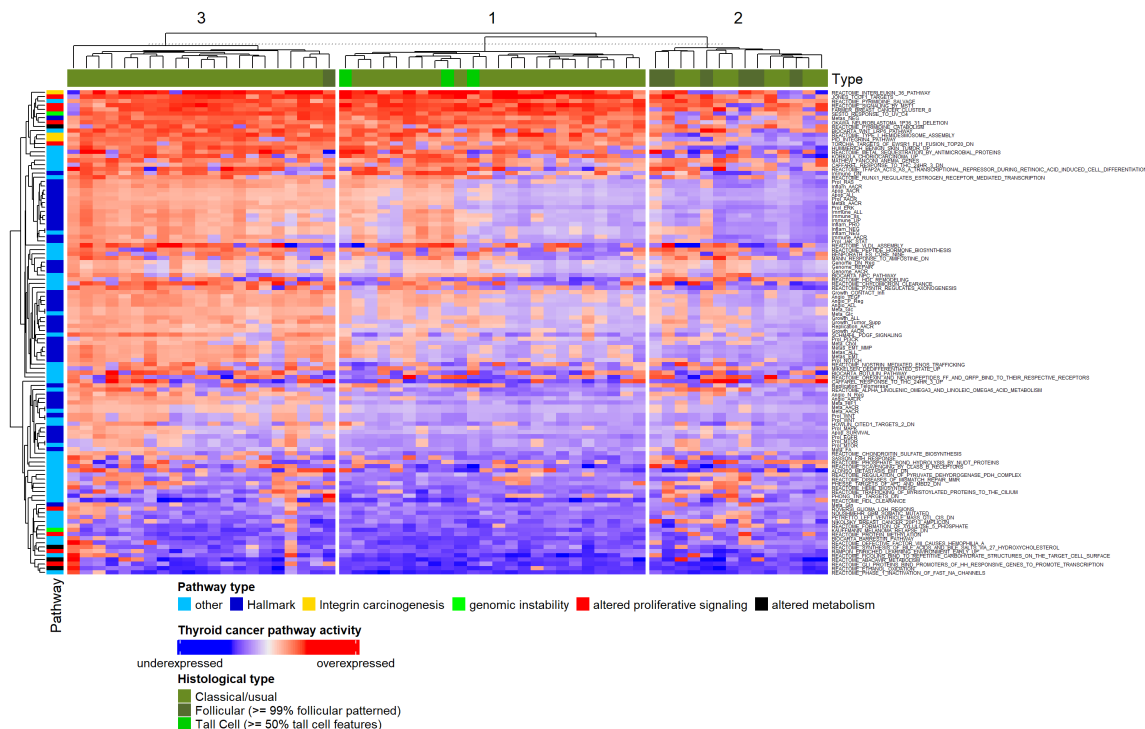

Figure 9: Pathway activity of the 50 most variant, hallmark, and 20 most significantly altered pathways for each patient. Column clusters were obtained by k-means clustering with k=3. Pathway activities were computed via GSEA of THCA expression data. For all pathway activities see figure (XXX in the apendix).

Regression analysis of THCA pathway activity

To select a suitable pathway for regression analysis, the top 20% pathways regarding their variance in activity were chosen, as for the regression model to predict. Pathways with little variance were found to be better predicted by a null model (Fig xxx supplementary material). To factor in biological significance, the intersect of the 25 most significantly altered pathways from GSVA with the high variance pathways was computed. This resulted in three significantly altered and highly variant pathways among which the REACTOME_INTERLEUKIN_36_PATHWAY gene set was selected. This gene set ranks 8th among the highest upregulated pathways with an associated p-value of 8.411155e-15. Interleukin 36 signaling is connected to both MAPK activity and through the activation of NF-kB and also the expression of integrin alpha6beta4.[@result4; @result7; @msigdb].

Regression of the REACTOME_INTERLEUKIN_36_PATHWAY gene set showed mixed results. After multiple testing an architecture with two hidden layers with 10 and 20 neurons respectively at ' set.seed(50) ' was shown to produce the best results for neuronal network regression. Among the tested models, the neuronal network performed best on the test data with a mean squared error (MSE) of 0.06. However, the linear regression model failed to predict the data accurately (MSE = 0.62). Repeated linear regression with just pathways contributing significantly to the result the performance was enhanced (MSE = 0.40), however, remained worse than a null model (MSE = +0.22). @ref(fig:reg) Comparison of the MSE on test

an training data reveals, that linear model is highly overfitted (ΔMSE = +0.55) with the linear model with significant pathways fitting slightly better (ΔMSE = +0.23) to the data. Our null model displayed an good, yet slightly underfitted performance with ΔMSE = -0.08. With a ΔMSE = +0.009 the neuronal network shows a perfect fit.

A comparison of the four regression models via the F-test function `var.test()` showed a significant improvement of the neuronal network compared to all other models. All other models showed no significant differences in their performance @ref(fig:reg) compared to each other. From this data, we can conclude that a neuronal network is the best choice for most accurately predicting IL-36 pathway activity in our test data.
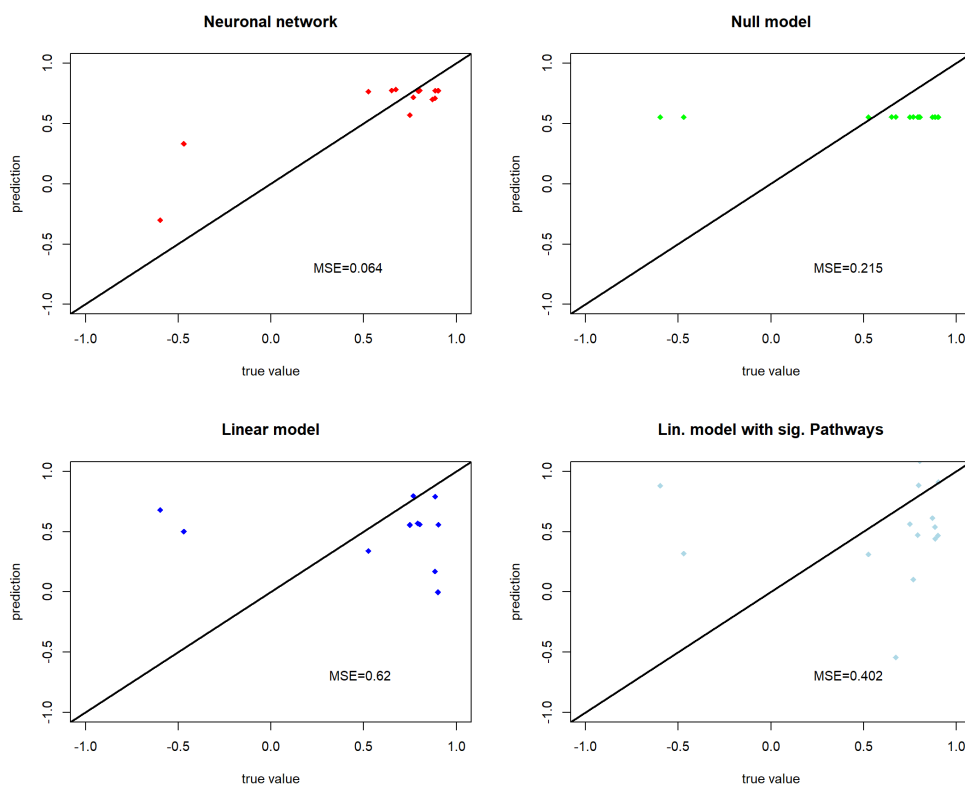

Figure 10: Regression results for various models on THCA GSEA test data. True values are plotted against predicted values, black slope indicate a perfect prediction.
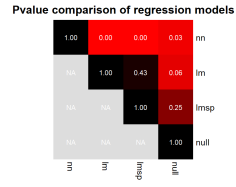
Figure 11: F-test comparison of various regression models. p-values are obtained from a two-sided variance test and displayed as heatmap. nn = neuronal network, lm = linear regression, lmsp = linear regression with only significant pathways, null = null model.